July 1992 *Chem. Pharm. Bull.* **40**(7) 1897—1901 (1992) 1897

Effect of Powder Addition to Carboxyvinylpolymer Hydrogel on Viscoelasticity

Shigeyuki Ishikawa* and Masao Kobayashi

Pharmaceutics Research Laboratory, Tanabe Seiyaku Co., Ltd., 16-89, Kashima 3-chome, Yodogawa-ku, Osaka 532, Japan.

Received December 9, 1991

The influence of the addition of powder on the viscoelasticity of carboxyvinylpolymer (CVP) hydrogel was studied by the oscillation method. The powder-filled hydrogels (PFHs) were prepared using Hiviswako 103 and 105 (CVP of rich side chains and poor side chains, respectively), and six powders [zinc oxide (ZnO), titanium dioxide (TiO_2), magnesium stearate (StMg), talc, synthetic aluminum silicate (SiAl), and hydrated silicone dioxide (Cp)].

The profiles of storage modulus (G') and loss modulus (G'') of each PFH differed depending on powder and CVP. $\log G'$ and $\log G''$ changed little with TiO_2, monotonously increased with talc, StMg and Cp, and showed fairly complex behaviors differing with polymer species with ZnO and SiAl. Plotting according to the Kerner equation suggested that powder bridge structures were formed in the PFHs.

The possible structures formed in the PFHs were presumed as follows on the basis of their viscoelasticity change and microscopic observation. With TiO_2: the original hydrogel network was not ruptured and powders were dispersed uniformly in the gel network. With talc, StMg and Cp: the original hydrogel networks and the powder bridge structures coexisted. With ZnO and SiAl: the original hydrogel networks were ruptured and powder bridge structures were constructed.

Keywords carboxyvinylpolymer; Hiviswako; powder; powder-filled hydrogel; viscoelasticity; oscillation method; powder property

In our earlier studies on the influence of powder addition on the rheological properties of vaseline and macrogol ointment (MGO),[1,2] the properties of the powder seemed to be reasonably shown on the former, but masked behind the thick surface adherence layers in MGO.

As ointment vehicles, hydrogels prepared by polymers such as carboxyvinylpolymer (CVP) have become popular because of their many advantages. To learn the effect of powder addition to such hydrogels is not only interesting from the physicochemical viewpoint but also useful for practical formulation studies. The viscoelasticity of these CVP hydrogels is thought to depend mainly on the expansion of the polymers due to the electric repulsive forces between carboxyl groups, and has such characteristics as less nonlinearity, less dependency on oscillation frequency, and rather small loss tangent [$\tan\delta$ = loss modulus (G'')/storage modulus (G')] compared to that of vaseline or MGO.[3]

We previously evaluated viscoelastic properties of six CVPs available in the market and found that Hiviswako 103 and 105 (denoted as H_{103} and H_{105}), respectively, show very different rheological behavior.[3] H_{103} gave high viscoelasticity and low intrinsic viscosity, while H_{105} gave low viscoelasticity and high intrinsic viscosity. We concluded the former to be a polymer consisting of rich side chains and the latter to be that with poor side chains.

Thus, these two polymers were used in this study, and 6 types of powders [zinc oxide (ZnO), titanium dioxide (TiO_2), synthetic aluminum silicate (SiAl), hydrated silicone dioxide (Cp), magnesium stearate (StMg), and talc] were added to the hydrogels, and the viscoelasticity of these powder-filled hydrogels (PFHs) was evaluated by the oscillation method as previously.

Experimental

Materials H_{103} and H_{105} (Wako Pure Chemical Industries., Ltd.) were used as received, and the same bulk batch was used as previously.[3] All the powders were obtained from commercial sources and the same bulk batches were used as previously.[1,2] Powder density (ρ), bulk density (ρ_{bulk}), specific surface area evaluated by the BET method (S_{BET}) and by the air permeability method (S_{AP}), and particle size determined by the Cilus method (D_{CL}) are shown in Table I.

Preparation of PFHs One gram of CVP was weighed rapidly in a 100 ml beaker and 30 ml of purified water was added to it under agitation with a glass bar, then allowed to settle about 1 h so that the polymer was well wetted. The powder was added under agitation, and an amount of 0.5 N NaOH necessary to adjust to pH 6 was added with slow agitation. Then, additional purified water was added to make 100 g of PFH and mixed well. The PFHs were stored in a tight-capped glassbottle at 25±1 °C until measured.

The reproducibility of the above PFH preparation was examined beforehand by repeating the preparation of some PFHs and evaluating viscoelasticity. The coefficients of variance (CV%) of $\log G'$ and $\log G''$ were 5.1% and 3.4% in the original gel (H_{103}, $n=10$), 5.7% and 2.6% in the 10% TiO_2-filled H_{103} hydrogel ($n=4$), and 4.1% and 4.1% in the 10% ZnO-filled H_{103} hydrogel ($n=4$), respectively.

Measurements of Viscoelasticity The oscillation measurement was carried out at 25±0.1 °C using a Shimadzu RM-1 rheometer as described previously[3] [cone angle (ε), 7×10^{-2} rad; strain amplitude (λ), 1.75×10^{-2} rad; radius of cone-plate (R), 2.5 cm; torsion constant of wire (K), 2.22×10^{6} dyne cm/rad; sample weight, about 3 g].

Rheological parameters G', G'', $\tan\delta$ and nonlinearity parameter (Dnl) were calculated using Eqs. 1—4, respectively. G' and G'' are indexes of solidity and liquidity, respectively. The loss tangent ($\tan\delta$) is regarded as an index of the relative contribution of liquidity and solidity to the stress. Dnl simply expresses the contribution ratio of total nonlinearity to the stress and is a convenient parameter by which to express the extent of the complication of the rheological behavior of the vehicle.[4]

$$G' = (3Ka_1/2\pi R^3)(\varepsilon/\lambda) \tag{1}$$

$$G'' = (3Kb_1/2\pi R^3)(\varepsilon/\lambda) \tag{2}$$

$$\tan\delta = G''/G' \tag{3}$$

Table I. Properties of the Powders Used in This Study

	ρ (g/cm^3)	ρ_{bulk} (g/cm^3)	S_{AP} (m^2/g)	S_{BET} (m^2/g)	D_{CL} (μm)	$r\cos\theta$
ZnO	5.74	0.46	1.57	3.33	1.1	1.36
TiO_2	3.97	0.52	2.85	8.93	0.6	a)
Cp	2.81	0.09	10.40	145.40	13.0	0.67
SiAl	2.41	0.17	5.52	417.05	11.1	1.07
StMg	1.10	0.26	1.69	4.69	15.6	0
Talc	2.82	0.40	1.23	2.17	12.9	0.52

a) Highly wetted.

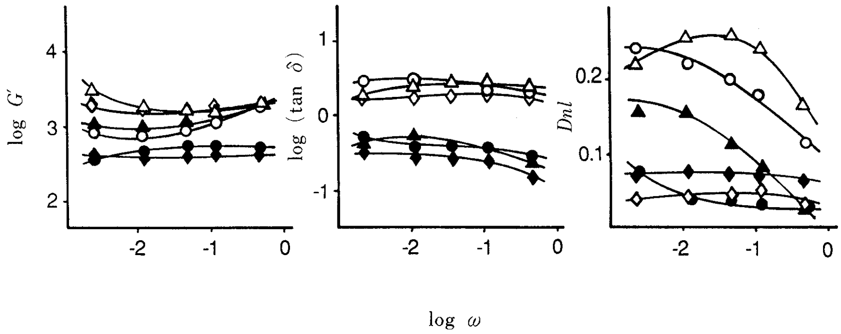

Fig. 1. Example of ω Dependency of G', tan δ and *Dnl* of Powder-Filled Hydrogels

Symbols: ◇, H_{103}; ◆, H_{105}; ○, TiO_2 (10%) in H_{103}; ●, TiO_2 (10%) in H_{105}; △, StMg (10%) in H_{103}; ▲, StMg (10%) in H_{105}.

$$Dnl=\left(\int_0^{2\pi}|\sigma_{\text{obs}}-\sigma_{\text{1st}}|d\theta\right)\Big/\left(\int_0^{2\pi}|\sigma_{\text{obs}}|d\theta\right) \quad (4)$$

where a_1 and b_1 are the first coefficients of the constitute wave in the Fourier series, and σ_{obs} and σ_{1st} are the obtained and calculated waves, respectively.[3)]

Wettability with Water Powders were packed into a glass capillary tube (diameter = 3.6 mm, length = 15 cm) and one side of the tube was immersed in purified water. The experiments were performed in a room where temperature was controlled at 25 °C. The rising liquid height (h) in the tube was measured and h^2 was plotted against time (t). The wettability ($r\cos\theta$) was calculated from Eq. 5 as previously:

$$h^2=(\gamma r\cos\theta)t/(2\eta) \quad (5)$$

where γ, r, η, and θ are surface tension, average capillary radius, viscosity of water and contact angle, respectively.

Results and Discussion

Powder Properties The powders used can be classified into the following 3 groups on the basis of their properties as earlier described.[1)]

1) Fine, high density, smooth surface, and little agglomeration (ZnO and TiO_2).

2) Porous, bulky density, and much coagulation of fines (SiAl and Cp).

3) Fairly large particle size, smooth surface, less coagulation, lubricating agent (StMg and talc).

Table I shows the wettability with water ($r\cos\theta$) of the powders used together with powder properties (ρ, ρ_{bulk}, S_{AP}, S_{BET}, D_{CL}). StMg had the poorest wettability. When the powder bed of TiO_2 was wetted, it immediately contracted when the water rose in the powder packed capillary tube, and the wetted bed then separated from the unwetted bed. Thus $r\cos\theta$ could not be evaluated, but the phenomenon qualitatively suggested that TiO_2 has the best water wettability among the 6 powders.

ω Dependency of Powder Filled Hydrogels As previously shown, $\log G'$ and $\log G''$ of CVP gels did not change greatly with oscillation frequency (ω) in the measurement range, while in other ointments such as MGO and vaseline they considerably differed with ω.[2,3)] In powder-filled hydrogels (PFHs) also, they did not change much with ω as shown by the examples in Fig. 1.

The nonlinearity parameter (*Dnl*) of the PFHs showed a different tendency from the original hydrogels. The *Dnl*s were small in both H_{103} and H_{105} hydrogels in the measured ω range. However, with the addition of powders, *Dnl*s increased at the lower ω range, and decreased at the higher ω range. The reducing tendency at high ω was common with other ointment vehicles. The large *Dnl* means that the PFHs generally have more thixotropic properties than the original hydrogels.[3)] According to Amari, nonlinearity is often observed in suspension and is attributable to construction and destruction of the internal structure produced by the dispersed powder.[5,6)] The larger *Dnl* of the PFHs would suggest that the structures are destroyed by shear-imposition but the reconstruction in the PFHs is more difficult than in the original hydrogels.

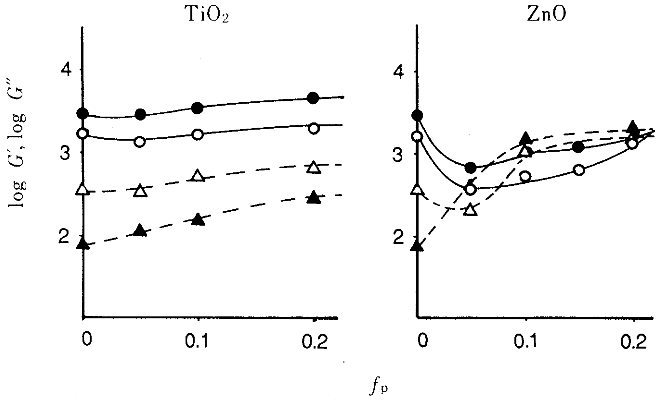

Fig. 2. Change of G' and G'' of PFHs with Weight Fraction of TiO_2 and ZnO

Symbols: ○, G' in H_{103}; ●, G'' in H_{103}; △, G' in H_{105}; ▲, G'' in H_{105}.

In the following section, the measurement of G' and G'' was performed at $\omega = 0.46$ rad/s as previously.[1,2)]

Influence of Powder Species and Their Amounts The profiles of $\log G'$ and $\log G''$ against the weight fraction of powder (f_p) are shown for the powder groups of 1, 2, and 3, from Fig. 2 to 4, respectively.

The addition of TiO_2 did not greatly change $\log G'$ and $\log G''$ in either polymer (H_{103} or H_{105}).

$\log G'$ of both polymers and $\log G''$ of H_{103} greatly decreased with the addition of ZnO at about $f_p = 0.05$ and thereafter increased monotonously, while $\log G''$ of H_{105} increased with increase of f_p without a decreasing phase. At $f_p = 0.2$, $\log G'$ and $\log G''$ of the two polymers were very similar to each other although the values of the original hydrogels greatly differed. This suggests that similar microstructures were formed in ZnO-filled hydrogels at high f_p irrespective of the difference in original hydrogels.

With the addition of Cp, $\log G'$ and $\log G''$ of both polymers increased monotonously with increase of f_p (Fig. 3). This tendency was similar to the case where Cp was

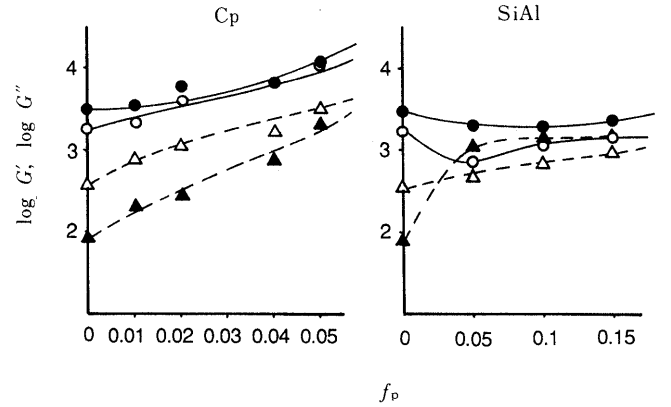

Fig. 3. Change of G' and G'' of PFHs with Weight Fraction of Cp and SiAl

Symbols same as in Fig. 2.

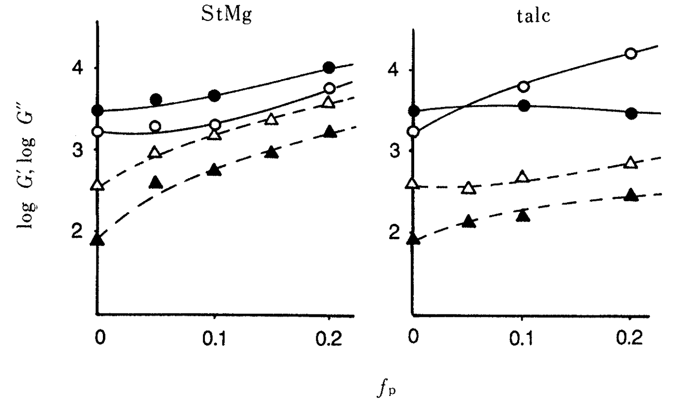

Fig. 4. Change of G' and G'' of PFHs with Weight Fraction of StMg and Talc

Symbols same as in Fig. 2.

added to vaseline or MGO.[1,2)]

The addition of SiAl caused the profiles of $\log G'$ and $\log G''$ to be quite different from the case of Cp. With H_{103}, $\log G'$ and $\log G''$ decreased at $f_p=0.05$, then increased slightly with increase of f_p. In H_{105}, however, $\log G'$ gradually increased with increase of f_p while $\log G''$ intensely increased up to $f_p=0.05$ and then the increase became gradual (Fig. 3). When f_p was over 0.1, $\log G'$ and $\log G''$ of both polymers became closer as ZnO-filled hydrogels.

The addition of StMg caused $\log G'$ and $\log G''$ of both polymers to monotonously increase with f_p (Fig. 4). The difference between $\log G'$ and $\log G''$ was almost the same at any f_p in the two polymers, meaning that G' and G'' change at the same rate, and $\tan\delta$ does not change much with the increase of f_p.

$\log G'$ and $\log G''$ of H_{105} increased a little with increase of f_p when talc was added (Fig. 4). However, $\log G'$ of H_{103} increased with increase of f_p, while but $\log G''$ of H_{103} scarcely changed.

Loss Tangent Figure 5 shows $\tan\delta$ of the PFHs [$(\tan\delta)_{PFH}$s] of H_{103} and H_{105} against the volume fraction of dispersed powders (ϕ_p) estimated from the densities of powders and the hydrogels.[3)]

If particles are rigid enough and no special interaction occurs between the hydrogels and the powders, the relative loss tangent, $(\tan\delta)_R$, can be written as:

$$(\tan\delta)_R=(\tan\delta)_{PFH}/(\tan\delta)_{HG}=1-\phi_p \tag{6}$$

where $(\tan\delta)_{HG}$ are $\tan\delta$ of the hydrogel.[1,7)] The values of theoretical $(\tan\delta)_R$ calculated from Eq. 6 are also shown for each PFH of H_{103} and H_{105}. The large difference between the theoretical and observed values suggests that the presumption of Eq. 6 is not satisfied and some interaction exists between the hydrogels and the powders.

The patterns of $(\tan\delta)_{PFH}$ can be classified as follows:

Case 1: The values are larger than the original gels in both H_{103} and H_{105} PFHs (StMg, TiO_2).

Case 2: The values once increased and then decreased in both polymers (ZnO, SiAl).

Case 3: The values increased in H_{105} but decreased in H_{103} (Cp, talc).

These behaviors seem concerned with the difference of the structures formed in the PFHs as will be discussed later.

Applicability of the Kerner Equation Raudebaugh and Simonelli reported the usefulness of the Kerner equation (Eq. 7) for a mixture in which the particles are sufficiently rigid compared with vehicles[7)]:

$$G'_R=1+\{15(1-\mu_1)/(8-10\mu_1)\}(\phi_2/\phi_1) \tag{7}$$

where μ_1, ϕ_1 (denoted as ϕ_{HG} in Fig. 6). and ϕ_2 (denoted

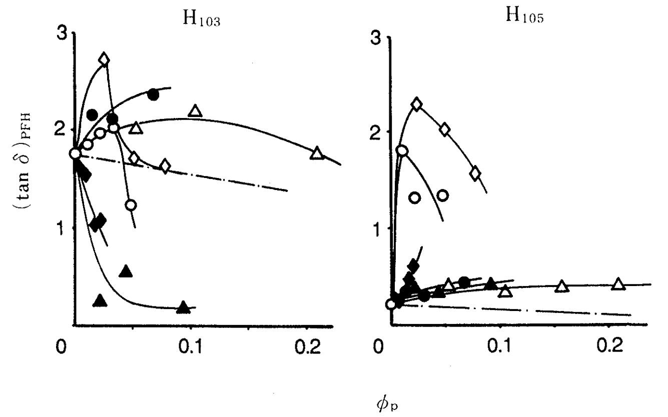

Fig. 5. Change of Loss Tangent of PFHs of H_{103} and H_{105} with Volume Fraction of Added Powders

Symbols: —·—: Theoretical values calculated from Eq. 6 for each PFH. ○, ZnO; ●, TiO_2; ◇, SiAl; ◆, Cp; △, StMg; ▲, talc.

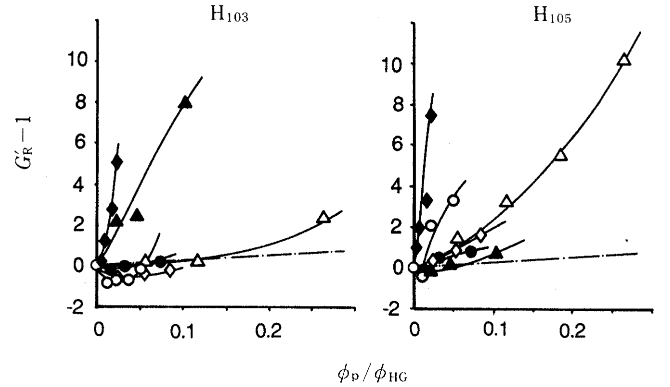

Fig. 6. Kerner Plots for Each Powder-Filled Hydrogel

Symbols same as in Fig. 5.

as ϕ_{p}) are Poisson's ratio of the bulk phase and volume fractions of hydrogel and powder, respectively. In Fig. 6, $G'_{\mathrm{R}}-1$ is plotted against $\phi_{\mathrm{p}}/\phi_{\mathrm{HG}}$ for H_{103} and H_{105} PFHs, respectively.

As shown in Fig. 6, the order of $(G'_{\mathrm{R}}-1)$s was as follows: Cp > talc > StMg > TiO_2 ≒ theoretical > ZnO ≒ SiAl (H_{103} PFHs) Cp > ZnO > StMg > SiAl > TiO_2 > talc > theoretical (H_{105} PFHs).

Raudebaugh and Simonelli suggested that G'_{R} should deviate to the higher values from the theoretical values if bridge structures are formed in the semisolid and should deviate to the lower values if slippage occurs under shear.[7)]

The values of $(G'_{\mathrm{R}}-1)$s higher than the theoretical values in Fig. 6 seem to indicate that powder bridge structures were formed in the PFHs. However, the values of H_{103} PFHs were lower than the theoretical values in ZnO and SiAl; but these seemed not to correspond to the slippage. The reason: If the slippage occurs, it seems to occur more frequently in the H_{105} PFHs than in the H_{103} PFHs since the original H_{105} gels are less viscoelastic than the original H_{103} gels. However, the values of $G'_{\mathrm{R}}-1$ of the H_{105} PFHs were higher than the theoretical values except at one point (ZnO, $\phi_{\mathrm{P}}/\phi_{\mathrm{HG}}=0.01$). This appeared to mean that the slippage hardly occurred in H_{105} PFH. Therefore, the possibility of slippage in the H_{103} PFHs should also be small and other reasons would be involved.

Influence of Interfacial Surface Area It is known that particle size affects the rheological behavior of a drug suspension.[8)] We showed that $\log G'$ or $\log G''$ of powder-filled MGO increased with increase of the interfacial surface area between the ointment vehicle and powders (S), irrespective of powder species.[2)] However, as shown in Fig. 7 for the H_{103} PFHs, the dependency of $\log G'$ on S was different from powder to powder. This tendency also held in the H_{105} PFHs (not shown).

The result suggests that a different mechanism that in MGO is attributable to the change in PFH viscoelasticity.

State of the Particle Dispersion Figure 8 shows microphotographs of representative powder (10%)-filled hydrogels of H_{103}.

Most TiO_2 particles seemed to disperse one by one and there was little coagulation (Fig. 8A). As previously shown, the coagulation of TiO_2 was great in vaseline.[1)] This difference could be due to the wettability of TiO_2 which is poor with hydrophobic mineral oil but is good with water (Table I).

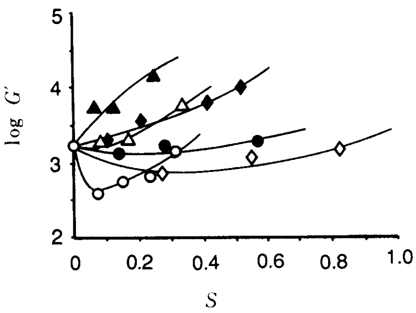

Fig. 7. Relationship between $\log G'$ of the H_{103} PFHs and Interfacial Surface Area between Particles and Vehicles

Symbols same as in Fig. 5.

ZnO coagulated more than to TiO_2 (Fig. 8B) although its powder properties were similar (Table I).

SiAl (Fig. 8C) and Cp (not shown) showed an almost similar dispersion situation with powders of irregular shapes thickly dispersed in all the spaces. Coagulated particles were observed in many fields and their extents in SiAl were greater than those in Cp.

Talc (Fig. 8D) and StMg (not shown) dispersed similarly. Fairly larger single particles were dispersed in all the spaces and coagulations were also observed in many fields, but coagulated particles were not as numerous as those of ZnO or SiAl.

Presumable Bridge Structure Formed in the PFHs From the above viscoelasticity and microscopic observations, the possible structures constructed in the PFHs were presumed to fall into the following 3 categories.

Case A: the particles are dispersed into single particles and are taken into the original hydrogel network without rupturing the network.

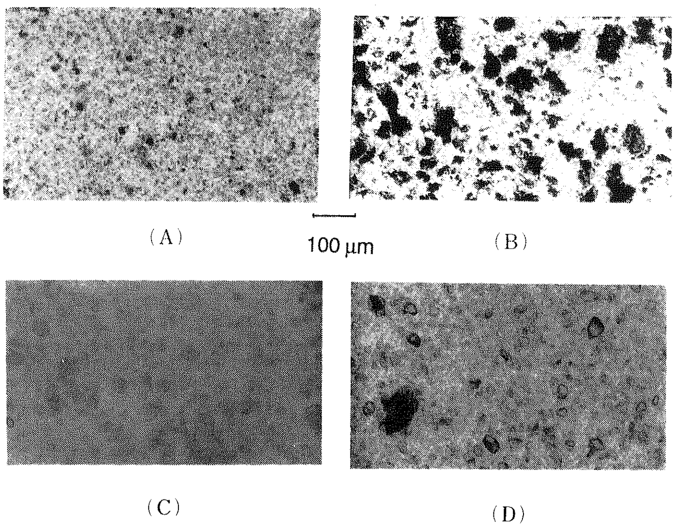

Fig. 8. Microphotographs of the H_{103} PFHs

A, TiO_2; B, ZnO; C, SiAl; D, talc.

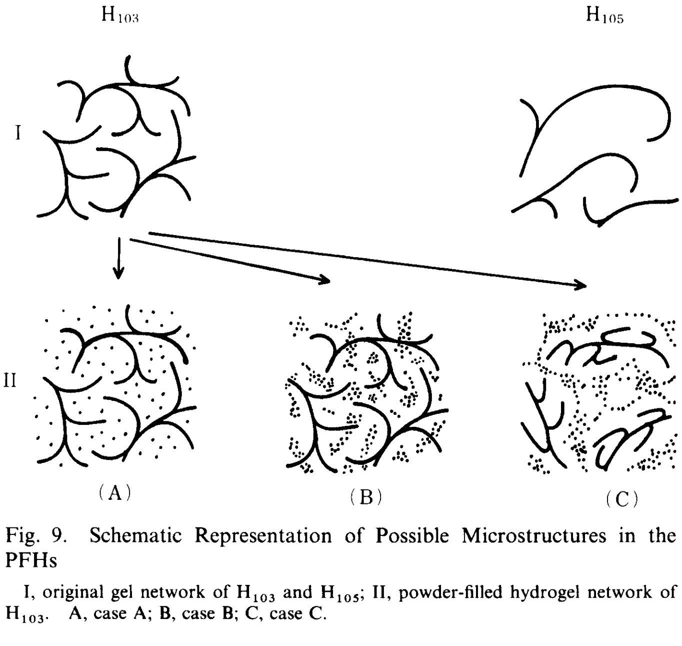

Fig. 9. Schematic Representation of Possible Microstructures in the PFHs

I, original gel network of H_{103} and H_{105}; II, powder-filled hydrogel network of H_{103}. A, case A; B, case B; C, case C.

Case B: the particles comprise a coagulated mass, and this mass is dispersed in the original hydrogel networks without rupturing the networks.

Case C: the original hydrogel networks are ruptured and the alternative bridge structures are constructed through coagulated powders.

The schemes of cases A, B, and C are shown in Fig. 9 for H_{103} PFHs. The scheme for H_{105} is the same as H_{103} except for the original polymer structure. The original polymer structure of H_{103} is richer in side chains than that of H_{105}.

The microstructure constructed in the PFH was presumed for each powder as follows:

TiO_2: case A seemed dominant. The small change of viscoelasticity in both polymers suggests that the dispersed powders did not affect the strength of the original hydrogel networks.

ZnO: the case C seemed dominant. The decrease of $\log G'$ at lower f_p in both polymers suggests that the original hydrogel network was ruptured. $\log G'$ and $\log G''$ of PFH were lower in H_{103} but were higher in H_{105} than the original hydrogel at higher f_p. This suggests that powder bridge structures are not as tough as the original network in H_{103}, while they are tougher than the original network in H_{105}. The fairly good agreement at higher f_p between H_{103} and H_{105} seemed to indicate that the produced powder bridge structures are similar.

Cp: cases A and B seemed to coexist and the latter to be more dominant. The monotonous increase of $\log G'$ and $\log G''$ with increase of f_p in both polymers suggests that the produced powder bridge structures contribute to the viscoelasticity as well as to the original hydrogel networks. The increase of $\log G'$ and $\log G''$ with f_p was more extensive in Cp than with StMg and talc. This could suggest that portion B is dominant in Cp due to the ease of entanglement of each powder because of their rough surface.

SiAl: case C seemed dominant. The decrease of viscoelasticity in H_{103} PFH, the increase in H_{105} PFH and the closeness each other at high f_p resemble the case of ZnO-filled hydrogels.

StMg: cases A and B seemed to coexist. The monotonous increases of $\log G'$ and $\log G''$ in both PFHs were the same as Cp. However, since the increase was not as great as in Cp, the portion case B seemed smaller in StMg than in Cp.

Talc: cases A and B seemed to coexist. The monotonous but very gradual increase of $\log G'$ and $\log G''$ in H_{105} suggests that case A is dominant. In H_{103}, $\log G'$ increased, but $\log G''$ hardly changed with f_p. This phenomenon is interesting but the reason is not yet clear.

As shown above, the patterns of viscoelasticity change in PFHs differed greatly depending on the powder added. The variety seemed the result of lesser compactness of the original hydrogel network. That is, the viscoelasticity is mostly determined by polymers whose weight fractions in the vehicles were very small (less than a few percent). Therefore, change in environmental factors could affect the viscoelasticity more easily than other ointment bases such as vaseline or MGO.

In ZnO and SiAl, polymers might be adsorbed by powders, so that the changing patterns of the viscoelasticity of the PFHs differed greatly depending on the polymer species.

On the contrary, in the case of talc, StMg, Cp, and TiO_2, the powders might not have much physicochemical interaction with the polymers. Thus, the polymer species apparently had little variable effect on the viscoelasticity, and the patterns of change of $\log G'$ and $\log G''$ were similar to each other in H_{103} and H_{105}.

References

1) S. Ishikawa, M. Kobayashi, and M. Samejima, *Chem. Pharm. Bull.*, **37**, 1355 (1989).
2) S. Ishikawa and M. Kobayashi, *Chem. Pharm. Bull.*, **38**, 2814 (1990).
3) S. Ishikawa, M. Kobayashi, and M. Samejima, *Chem. Pharm. Bull.*, **36**, 2118 (1988).
4) M. Kobayashi, S. Ishikawa, and M. Samejima, *Chem. Pharm. Bull.*, **30**, 4468 (1982).
5) T. Amari, *Nippon Rheology Gakkaishi*, **14**, 167 (1986).
6) T. Amari and K. Watanabe, *Nippon Rheology Gakkaishi*, **14**, 37, (1986).
7) G. W. Raudebaugh and A. P. Simonelli, *J. Pharm. Sci.*, **73**, 590 (1984).
8) S. S. Ober, H. C. Vincent, D. F. Simon, and K. J. Frederick, *J. Am. Pharm. Assoc.*, **47**, 667 (1958).